THE JOURNAL OF PHYSICAL CHEMISTRY B LETTERS

2006, *110,* 10220−10223
Published on Web 05/12/2006

Microscopic Folds and Macroscopic Jerks in Compressed Lipid Monolayers

A. Gopal,[†] V. A. Belyi,[‡] H. Diamant,*[,§] T. A. Witten,[‡] and K. Y. C. Lee[†]

Department of Chemistry, James Franck Institute, Institute for Biophysical Dynamics, and Department of Physics, University of Chicago, Chicago, Illinois 60637, and School of Chemistry, Beverly & Raymond Sackler Faculty of Exact Sciences, Tel Aviv University, Tel Aviv 69978, Israel

Received: March 27, 2006; In Final Form: April 27, 2006

We report hitherto unrecognized cooperative behavior in the stochastic collapse of certain compressed lipid monolayers implicated in pulmonary function. The cooperativity emerges from a statistical analysis of the collapse events captured using fluorescence microscopy and digital image analysis. The collapse events involve folding of the monolayer on a micron scale, yet each event produces a macroscopic jerk of the layer. The cooperative collapse is striking for its temporal sharpness and large spatial extent.

1. Introduction

As one knows from everyday experience, when a flat thin sheet of material is subjected to increasing lateral pressure, it will eventually either buckle or break. A monolayer of surface-active molecules adsorbed on a liquid interface is an extreme example of a thin sheet. Such surfactant monolayers are found in many systems containing water−air or water−oil interfaces where surface tension, wetting, or liquid film stability are to be controlled.[1] The failure of these layers is a distinctive mechanical regime as well as a practically important phenomenon, for instance, in the function of lungs.[2−4]

Buckling[5,6] and fracturing[7,8] were both observed in compressed surfactant monolayers. In recent years, however, a remarkable variety of other structures have been discovered in laterally compressed monolayers, including straight folds,[9−13] convoluted giant folds,[11,14] and vesicular objects of various shapes.[10,15] Unlike buckling and fracturing, which correspond to two extremes with regard to the length scale of response (the former occurring over macroscopic distances and the latter involving the breakage of microscopic bonds), those recently observed structures have distinctive mesoscopic length scales ranging between 0.1 and 10 μm.

Of these structures, the straight folds are of particular interest, since they lead to a sudden, irreversible release of energy, corresponding to a far-from-equilibrium response of the layer.[9−13] The folds, which have been observed in several different systems, seem to occur in groups.[11,12] Each fold comprises a piece of monolayer of micron width and macroscopic length bound into a bilayer strip (Figure 1a). The fold is randomly nucleated at a defect—either at a grain boundary (in single-phase monolayers)[11] or a domain boundary (in biphasic ones)[10,16,17]—and takes a fraction of a second to form. Hence, its actual formation is very rarely captured inside the microscope field of view. We observed, nonetheless, that whenever a fold forms outside the field of view a large area of the monolayer jerks, i.e., translates sharply and uniformly. (See Figure 1b and the video provided as Supporting Information.) Hence, we devised a technique combining fluorescence microscopy and digital image analysis to follow such jerks and thereby gain insight into this peculiar mode of collapse.

2. Experimental Methods

The investigated monolayer is made of a mixture of two insoluble phospholipids, dipalmitoylphosphocholine (DPPC) and palmitoyloleoylphosphoglycerol (POPG), in 7:3 ratio, at 25 °C. These molecules constitute a good model system for the lipid components in the lung surfactant. The mixture is spread over a water−air interface on a rectangular Langmuir trough of maximum area 145 cm^2. The trough is fitted with two mobile barriers of length 6.35 cm each, allowing for symmetric lateral compression. The relative barrier velocity is 0.1 mm/s, corresponding to a strain rate of 1.5×10^{-3} s^{-1} at the onset of collapse. The area per molecule at this point is about 30 Å^2. Throughout the compression, the morphology is observed using epifluorescence video microscopy and the surface pressure monitored by a Wilhelmy surface balance. (Further details of the apparatus can be found in ref 10.)

The analogue epifluorescence video of monolayer motion is digitized into a series of 8-bit gray scale bitmaps of 640 × 480 pixels at a rate of 29.97 frames/s. The series of images are subsequently analyzed using a custom-made tracking program whose output is the two-dimensional velocity of the monolayer as a function of time. The program achieves a spatial precision of $^1/_9$ of a pixel by independently tracking separate regions of the image. A collapse event is identified by a velocity threshold of 2 pixels per frame (20.6 μm/s). The beginning of the identified event is found by going back until the change in velocity (i.e., acceleration) exceeds a threshold of 0.7 pixel/frame^2 (216 μm/s^2). Similarly, the end of the event is identified by first locating the frame of threshold velocity on the other

* Corresponding author. E-mail: hdiamant@tau.ac.il.
[†] Department of Chemistry, James Franck Institute, and Institute for Biophysical Dynamics, University of Chicago.
[‡] James Franck Institute and Department of Physics, University of Chicago.
[§] Tel Aviv University.

10.1021/jp0618983 CCC: $33.50

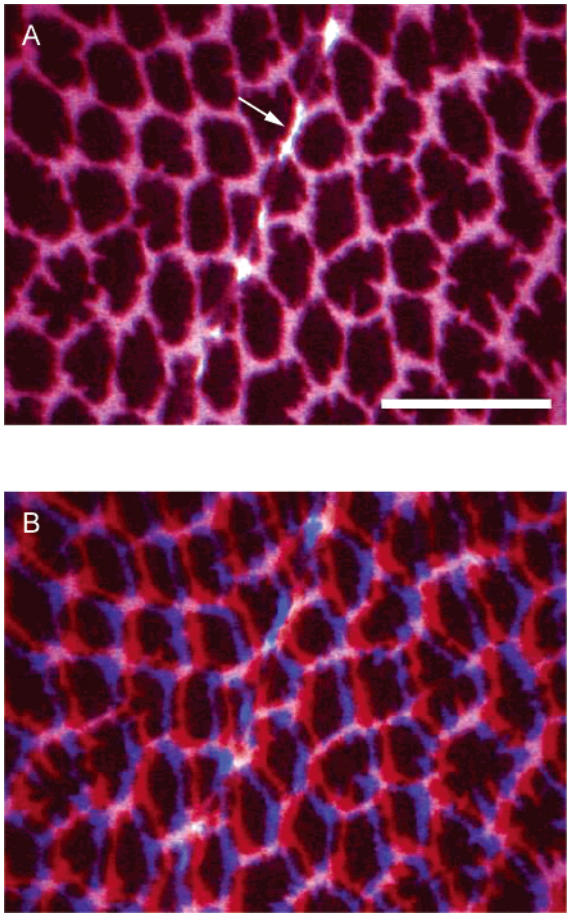

Figure 1. (a) Fluorescence micrograph of the compressed lipid monolayer after the onset of folding, exhibiting a biphasic structure of condensed domains (black) in a more liquid phase (purple). The bright streak indicated by an arrow is a preformed fold, projecting stronger fluorescence per unit area than the surrounding layer. The scale bar length is 50 μm. The image is actually an overlay of two micrographs taken $^1/_6$ s apart, one rendered in red and the other in blue, to demonstrate a stationary monolayer. (b) A similar overlay of two micrographs of the same region, separated again by $^1/_6$ s, yet demonstrating in this case a coherent jerk due to folding outside the field of view.

side of the velocity spike and then going forward until the deceleration goes beyond a threshold of -0.7 pixel/frame^2. Having identified an event, we record its starting point, duration, and total two-dimensional translation.

3. Results

For surface pressures higher than 15 mN/m, the monolayer exhibits a biphasic structure of condensed domains surrounded by a more liquid phase (Figure 1a). Collapse sets in at a pressure of 71 mN/m, whereupon the monolayer starts to jerk. (See Figure 1b and video in the Supporting Information.) Image analysis of the epifluorescence video frames yields the two-dimensional velocity of the monolayer as a function of time.

A typical output signal is presented in Figure 2 as a "seismogram", showing the jerks as velocity spikes and highlighting the striking abruptness of the phenomenon. We have identified 1817 events, recording for each its starting time, duration T, and total translation $\vec{l} = (l_x, l_y)$. The large amount of data allows, for the first time, a reliable analysis of the collapse dynamics, leading to several surprising observations as presented below.

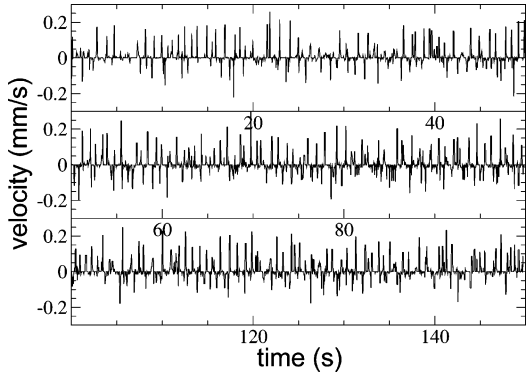

Figure 2. A typical image analysis signal presented as a "seismogram". Shown is the monolayer velocity parallel to the direction of compression as a function of time. The spikes correspond to jerks resulting from out-of-view folding events. Note the large variance of spike heights as compared to their well-defined rate and duration. The asymmetry between positive and negative translations arises from the asymmetric position of the field of view with respect to the two barriers.

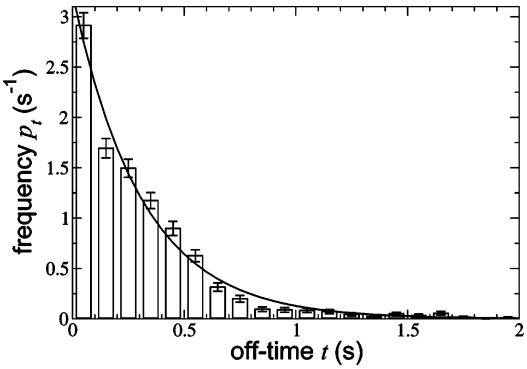

Figure 3. Distribution of off-times. The solid line shows an exponential distribution, $p_t(t) = \langle t \rangle^{-1}\, e^{-t/\langle t \rangle}$, using the measured mean off-time $\langle t \rangle = 0.31$ s.

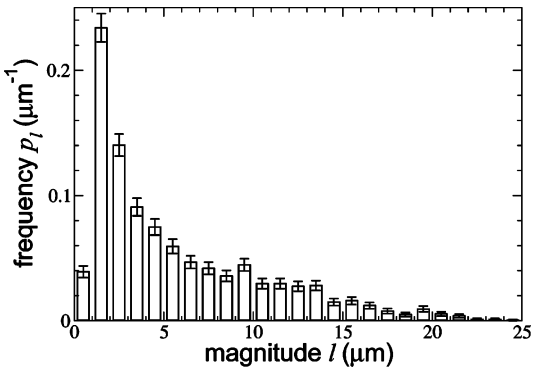

Figure 4. Distribution of jerk magnitudes (total translation during a jerk). Note the finite probability of having very large jerks.

Figure 3 shows the distribution of off-times t (waiting times between events). The mean off-time is $\langle t \rangle = 0.31 \pm 0.01$ s, i.e., there are about three events per second. The histogram fits well an exponential distribution, $p_t(t) = \langle t \rangle^{-1}\, e^{-t/\langle t \rangle}$, consistent with a Poissonian, uncorrelated sequence of events. We further confirmed the lack of correlation between the jerk magnitude (its total translation) and the off-times preceding or following it. Comparison between the measured rate of jerks and the typical rate at which folding events fall inside the field of view reveals that each fold creates a jerk extending over much of the macroscopic sample.

The distribution of jerk magnitudes is presented in Figure 4. It is anomalously broad—while the most probable jump spans

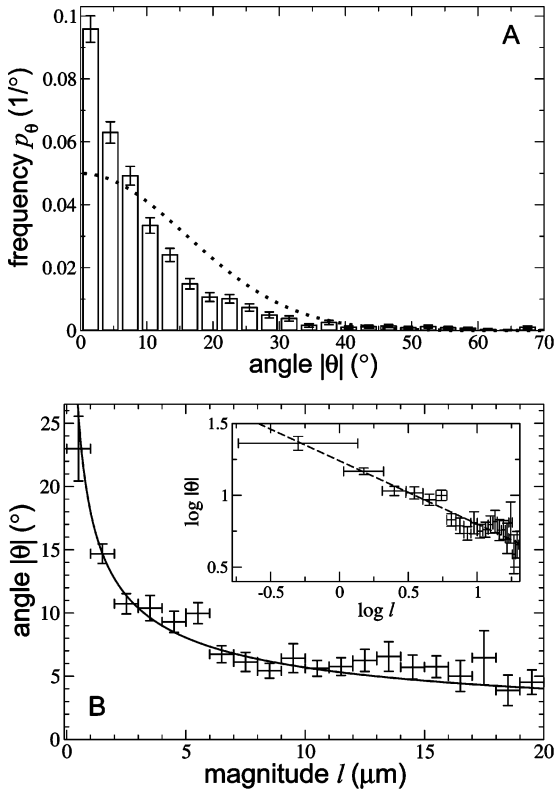

Figure 5. (a) Distribution of jerk angles. The dotted line shows a Gaussian distribution with the measured standard deviation. (b) Correlation between jerk angle and jerk magnitude. The solid line is a fit to $|\theta| = al^{-1/2}$ with $a = 18 \pm 3$ (°) $\mu m^{1/2}$. The inset presents the same data on a log−log scale, the dashed line being an error-weighted linear fit with a slope of -0.44 ± 0.05.

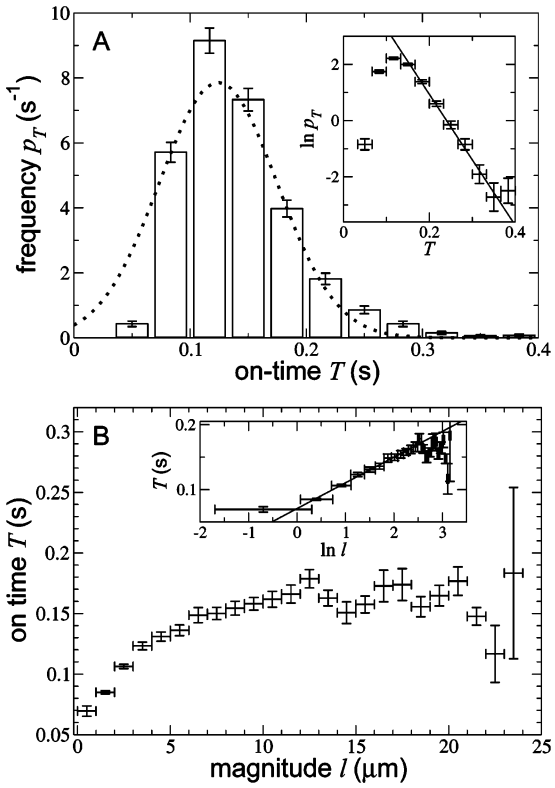

Figure 6. (a) Distribution of on-times (jerk durations). The dotted line shows a Gaussian distribution using the measured mean and standard deviation. The inset presents the data on a linear−ln scale, demonstrating an exponential distribution to the right of the peak. The solid line is an error-weighted linear fit with a slope of -23.3 ± 3 s^{-1}. (b) Correlation between the on-time and jerk magnitude. The inset presents the same data on a ln−linear scale, demonstrating a logarithmic dependence. The solid line is an error-weighted linear fit with a slope of 0.040 ± 0.004 s.

about 2 μm, translations 10 times that value were observed. This is vividly reflected also in the large variance of spike heights in the "seismogram" of Figure 2.

Figure 5a shows the distribution of absolute jerk angles $|\theta|$, obtained from the measured translation as $\tan \theta = l_y/l_x$. (Zero angle corresponds to motion parallel to the compression direction.) The angular distribution is sharply peaked at $\theta = 0$, with standard deviation $\sigma_\theta = 16.0 \pm 0.3°$. Folding is thus highly anisotropic, showing that these monolayers can support anisotropic stress like an elastic solid during the off-times between events (a few tenths of a second). This solidlike behavior is in line with the viscoelasticity revealed by surface-rheology measurements in similar systems.[14,18] The peak of the measured angular distribution is anomalously sharp and cannot be fitted by a normal Gaussian distribution (dotted curve in Figure 5a). In Figure 5b, we show the correlation between the jerk angle $|\theta|$ and the jerk magnitude l. The two quantities are anticorrelated—larger jerks have smaller angles—their interdependence following an inverse-square-root law, $|\theta| \sim l^{-1/2}$.

In Figure 6a, we present the distribution of on-times, i.e., jerk durations T. Unlike the magnitude distribution the on-time distribution is narrow, with a mean on-time $\langle T \rangle = 0.124 \pm 0.001$ s and standard deviation $\sigma_T = 0.051 \pm 0.001$ s. The distribution is asymmetric. (The corresponding Gaussian distribution is depicted by the dotted line.) The more moderate decrease to the right of the peak fits an exponential decay rather than a Gaussian one (Figure 6a inset). The correlation between T and l, drawn in Figure 6b, shows the expected increasing correspondence—larger jerks take a longer time. Yet, the increase is very weak, following a logarithmic law (Figure 6b inset). Thus, much larger jerks do not have a correspondingly long duration. The fact that jerks of largely differing magnitudes have similar durations is consistent with the surprising contrast between the breadth of the magnitude distribution (Figure 4) and the narrowness of the on-time distribution (Figure 6a).

4. Discussion

One of our key findings is the anomalously broad distribution of jerk magnitudes (Figure 4). It has become clear from various observations of the folding phenomenon[10−12] that the collapse evolves through groups of similar folds. (In the systems of refs 11 and 12, the distances between neighboring folds are smaller than in ours, making the multiple folding more apparent.) Such observations would suggest a narrowly peaked distribution of jerk magnitudes, in contrast to the broad distribution we observed. A plausible resolution of this puzzle would be to interpret each observed jerk as a *cascade* of folds, where the cascades have a broad distribution of magnitudes.

Furthermore, a detailed analysis of the statistical distributions presented above shows that they are fully consistent with a description of cooperative folding cascades occurring in a chain-reaction manner. In such a description, the properties of an individual fold (magnitude, angle, on-time) are normally distributed. Each fold, however, may "topple" several next-generation folds, and each of those may topple additional folds, up to g generations in a cascade.

For instance, the anomalous narrowing of the angular distribution (Figure 5a) follows from the fact that the observed jerk angle is actually an average over individual fold angles

which are normally distributed. The larger the cascade, the larger is the number of individual angles participating in the averaging, leading to a narrower distribution around $\theta = 0$. This readily accounts for the anticorrelation between magnitude and angle, obeying a $|\theta| \sim l^{-1/2}$ law as in Figure 5b. In a chain-reaction process, the magnitude (number of folds) grows exponentially with the number of generations g in the cascade, while the duration increases only linearly with g. This leads to a weak, logarithmic dependence between T and l, as in Figure 6b. Since, in the simplest description, g should be exponentially distributed, and l depends exponentially on g, the distribution of magnitudes should exhibit a long (power-law) tail for large l, as in Figure 4.

Using such a simple chain-reaction model, we have been able to fit the measured distributions and extract the various parameters characterizing the cascades. The translation "quantum", corresponding to a single fold, is 2.0 ± 0.8 μm. The single-fold duration is 0.12 ± 0.03 s. This value agrees with the total duration of a single fold, on the order of 0.1 s, observed in a different lipid mixture.[12] The cooperativity parameter is 1.9 ± 0.2, i.e., each fold topples on average about two others in the next generation. The toppling time between consecutive generations is only 0.026 ± 0.005 s, which is much shorter than the single-fold duration. This explains why the cascades appear as continuous jerks rather than series of discrete jumps.

5. Conclusion

The measured statistics of folding dynamics suggest that the collapse of the compressed lipid monolayer evolves through cooperative cascades of discrete folds. This new type of thin-layer failure is not restricted to our specific lipid mixture or its biphasic structure.[11,12] Moreover, a similar fold-and-jerk behavior has recently been observed in lipid monolayers covering microbubbles, where the monolayer area is on the order of 10^2 μm^2, and the compression caused by bubble shrinkage is isotropic.[13] Thus, the phenomenon analyzed here may be relevant to a host of natural scenarios including the compressed surfaces of air sacs in the lung.

From a yet broader perspective, the cascades represent unusual nucleation kinetics, in which single-fold growth is macroscopic in one dimension (length) but restricted in another (width). Consequently, a single nucleus cannot fully relax its overstressed environment, thereby leading to the nucleation of other folds in a chain-reaction manner. Such a process, resembling an autocatalytic chemical reaction or nuclear fission, has never been recognized, to our knowledge, in the context of mechanical instability such as the folding discussed here. Furthermore, this scenario should not be restricted to monolayer folding but is to be expected whenever there is an autocatalytic instability whose evolution is limited for some reason to discrete units of relaxation.

This study should be extended in several directions. Higher time resolution is required to resolve the individual folds in a cascade and confirm our statistical inferences. The dependence on various physical parameters, such as compression rate, monolayer composition, and viscosity of the subphase, should be explored to see whether the phenomenon can be made even more dramatic. These experiments are underway.

Acknowledgment. We thank D. Andelman and J. Klafter for helpful discussions. This work was supported by the US−Israel Binational Science Foundation (2002-271) and the University of Chicago MRSEC program of the NSF (DMR-0213745). The experimental apparatus was made possible by an NSF CRIF/Junior Faculty Grant (CHE-9816513). K.Y.C.L. is grateful for support from the March of Dimes (#6-FY03-58) and the Packard Foundation (99-1465).

Supporting Information Available: Movie of the unstable monolayer of Figure 1, showing the abrupt jerks and formation of a fold. This material is available free of charge via the Internet at http://pubs.acs.org.

References and Notes

(1) Birdi, K. S. *Self-Assembly Monolayer Structures of Lipids and Macromolecules at Interfaces*; Plenum Press: New York, 1999.
(2) Lipp, M. M.; Lee, K. Y. C.; Zasadzinski, J. A.; Waring, A. J. *Science* **1996**, *273*, 1196−1199.
(3) Lipp, M. M.; Lee, K. Y. C.; Waring, A. J.; Zasadzinski, J. A. *Biophys. J.* **1997**, *72*, 2783−2804.
(4) Kurutz, J. W.; Diamant, H.; Jiarpinitnun, C.; Waring, A. J.; Lee, K. Y. C. In *Lung Surfactant Function and Disorder*; Nag, K., Ed.; Lung Biology in Health and Disease Series, Vol 201; Marcel Dekker: New York, 2005.
(5) Saint-Jalmes, A.; Graner, F.; Gallet, F.; Houchmandzadzeh, B. *Europhys. Lett.* **1994**, *28*, 565−571.
(6) Saint-Jalmes, A.; Gallet, F. *Eur. Phys. J. B* **1998**, *2*, 489−494.
(7) Pauchard, L.; Meunier, J. *Phys. Rev. Lett.* **1993**, *70*, 3565−3568; *Philos. Mag. B* **1998**, *78*, 221−224.
(8) Hatta, E.; Hosoi, H.; Akiyama, H.; Ishii, T.; Mukasa, K. *Eur. Phys. J. B* **1998**, *2*, 347−349.
(9) Lipp, M. M.; Lee, K. Y. C.; Takamoto, D. Y.; Zasadzinski, J. A.; Waring, A. J. *Phys. Rev. Lett.* **1998**, *81*, 1650−1653.
(10) Gopal, A.; Lee, K. Y. C. *J. Phys. Chem. B* **2001**, *105*, 10348−10354.
(11) Ybert, C.; Lu, W.; Möller, G.; Knobler, C. M. *J. Phys. Chem. B* **2002**, *106*, 2004−2008; *J. Phys. Condens. Matter* **2002**, *14*, 4753−4762.
(12) Zhang, Y.; Fischer, T. M. *J. Phys. Chem. B* **2005**, *109*, 3442−3445.
(13) Gang, P.; Borden, M. A.; Longo, M. L. *Langmuir* **2006**, *22*, 2993−2999.
(14) Lu, W.; Knobler, C. M.; Bruinsma, R. F.; Twardos, M.; Dennin, M. *Phys. Rev. Lett.* **2002**, *89*, 146107.
(15) Nguyen, T. T.; Gopal, A.; Lee, K. Y. C.; Witten, T. A. *Phys. Rev. E* **2005**, *72*, 051930.
(16) Diamant, H.; Witten, T. A.; Gopal, A.; Lee, K. Y. C. *Europhys. Lett.* **2000**, *52*, 171−177.
(17) Diamant, H.; Witten, T. A.; Ege, C.; Gopal, A.; Lee, K. Y. C. *Phys. Rev. E* **2001**, *63*, 061602.
(18) Kragel, J.; Li, J. B.; Miller, R.; Bree, M.; Kretzschmar, G.; Mohwald, H. *Colloid Polym. Sci.* **1996**, *274*, 1183−1187.